# Numerical simulation of transport and noise in mesoscopic cavities

**M. Macucci**

*Dipartimento di Ingegneria dell'Informazione*

*Via Caruso 16, I-56122, Pisa, Italy.*

*macucci@mercurio.iet.unipi.it*

Coworkers: G. Iannaccone, P. Marconcini, M. Girlanda, L. Bonci

# Summary

- Tunneling enhancement due to a mesoscopic cavity
- Numerical methods for transport and noise
- Application to shot noise suppression in cavities as a function of constriction width and of magnetic field
- Dependence of the Fano factor on cavity length
- Open issues on multiple cascaded cavities
- Optimization of electronic structure calculations for carbon nanotubes
- Conclusions

# Structure of a mesoscopic (or chaotic) cavity

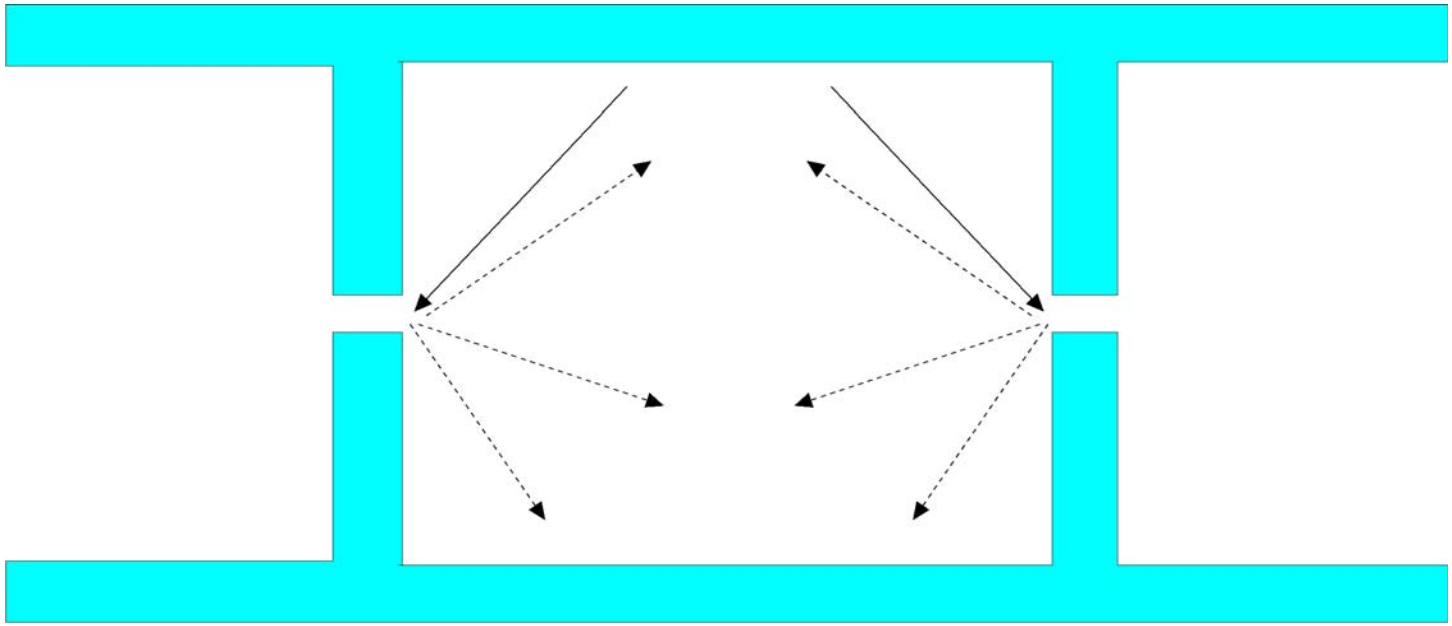

**A mesoscopic cavity is a region with a size of a few square micrometers, but delimited my nanoscale constriction (a few tens of nanometers wide)**

# Transmission of a cavity with a potential barrier

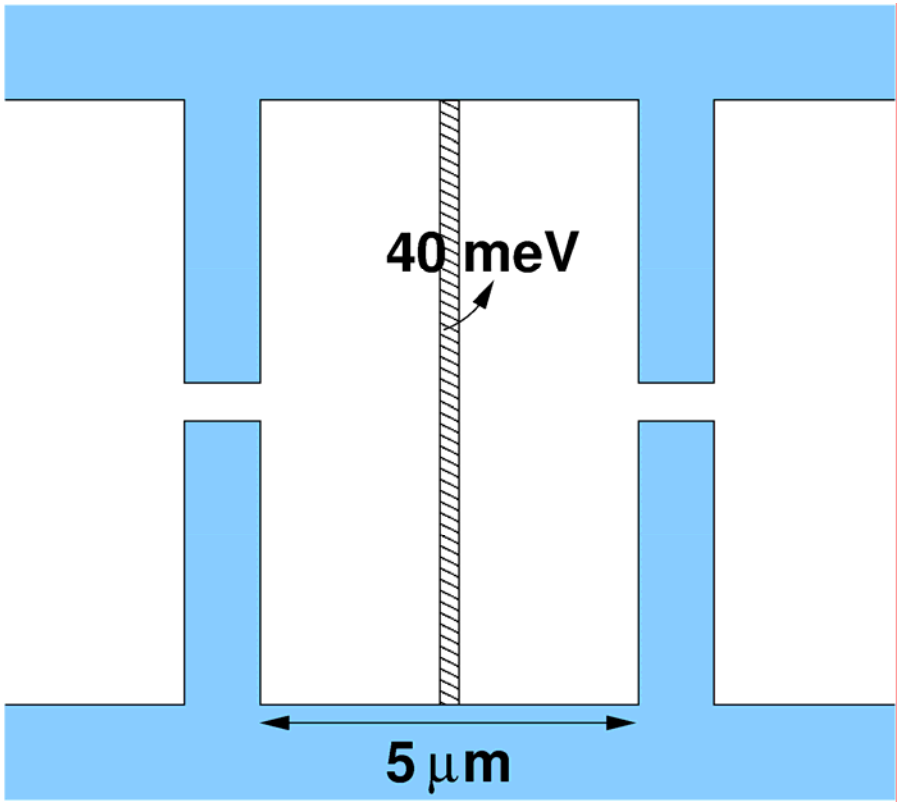


- Enclosing a barrier in a mesoscopic cavity has unexpected effects on its transparency
- Transmission is greatly enhanced if the barrier is exactly in the middle of the cavity
- We have examined several combinations of parameters, in order to understand the origin of this phenomenon

# Conductance in the case of a 4 micron wide cavity

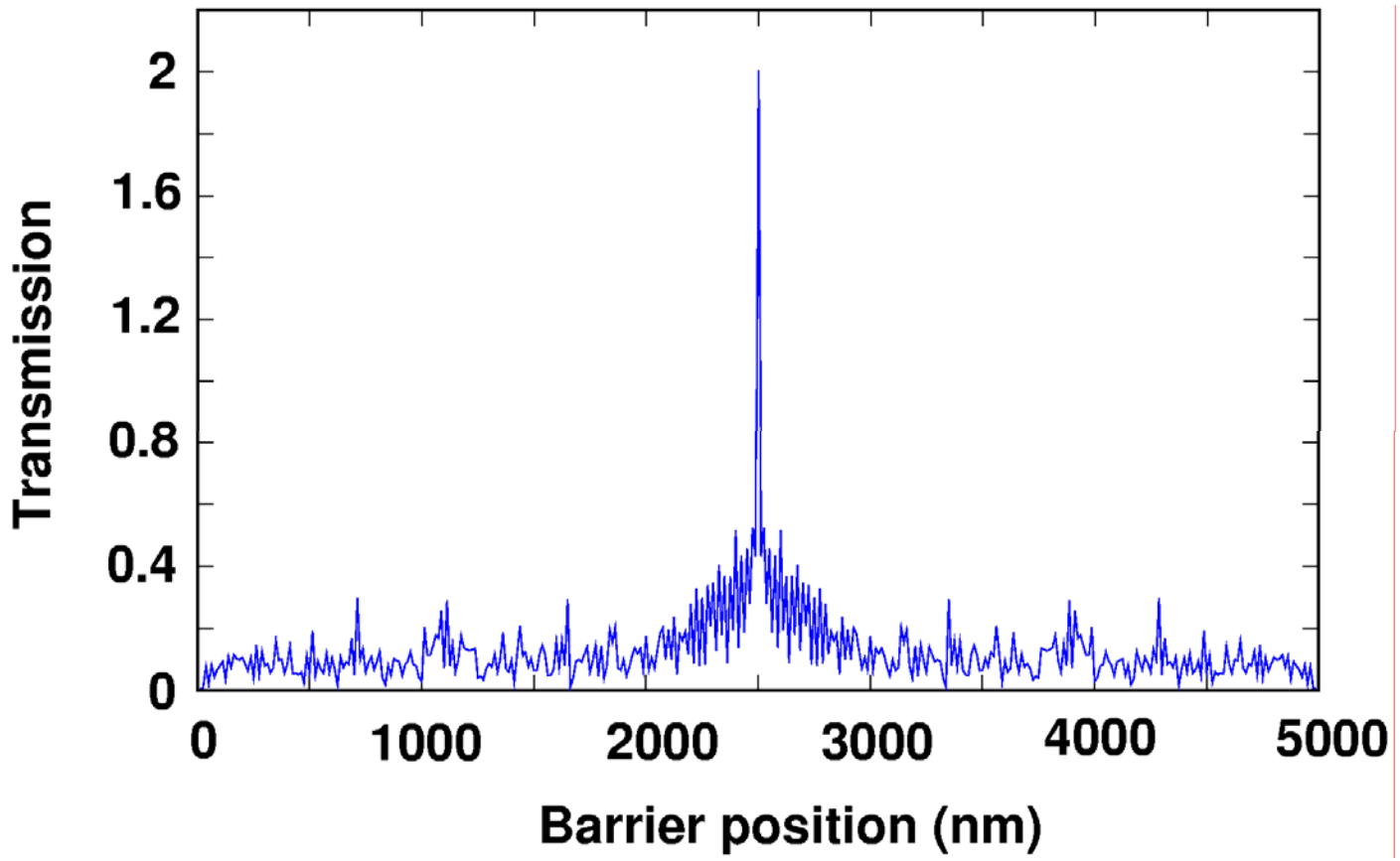


For 125 nm constrictions and a 5 μm long cavity, we observe a peak conductance of about 2 $G_0$, although the barrier alone would have a conductance of 0.244 $G_0$, when inserted in a 4 μm wide waveguide

# Effect of constriction asymmetry

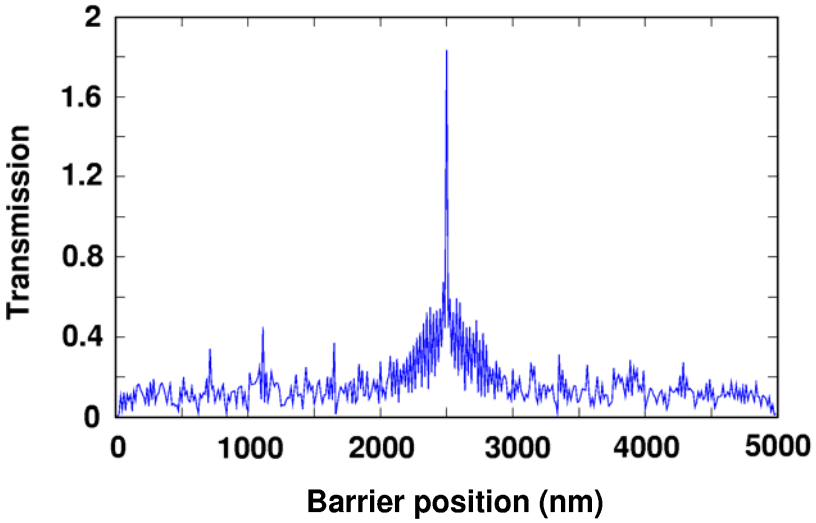


a)

**Unequal width**

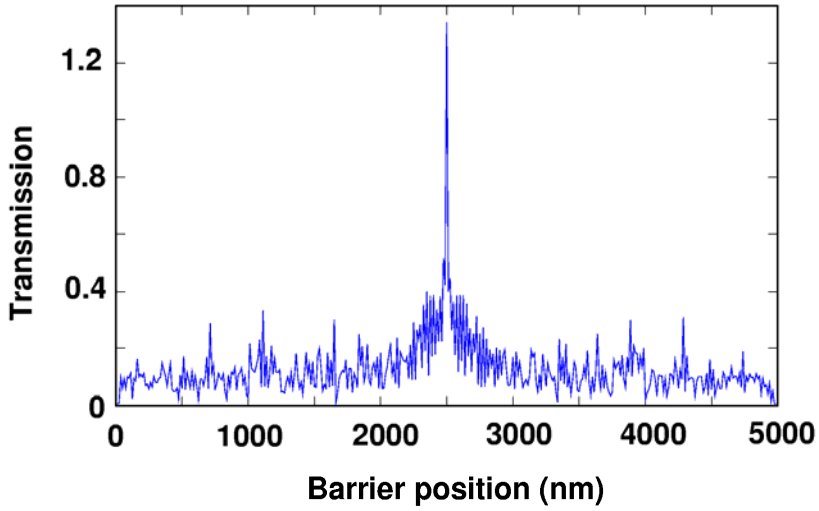


b)

**Shifted constrictions**

- **The tunneling enhancement effect survives the introduction of asymmetries in terms of constriction widths or of constriction position in the vertical direction**
- **This suggests that it is not a resonance effect**

# Conductance in the case of a 500 nm wide cavity

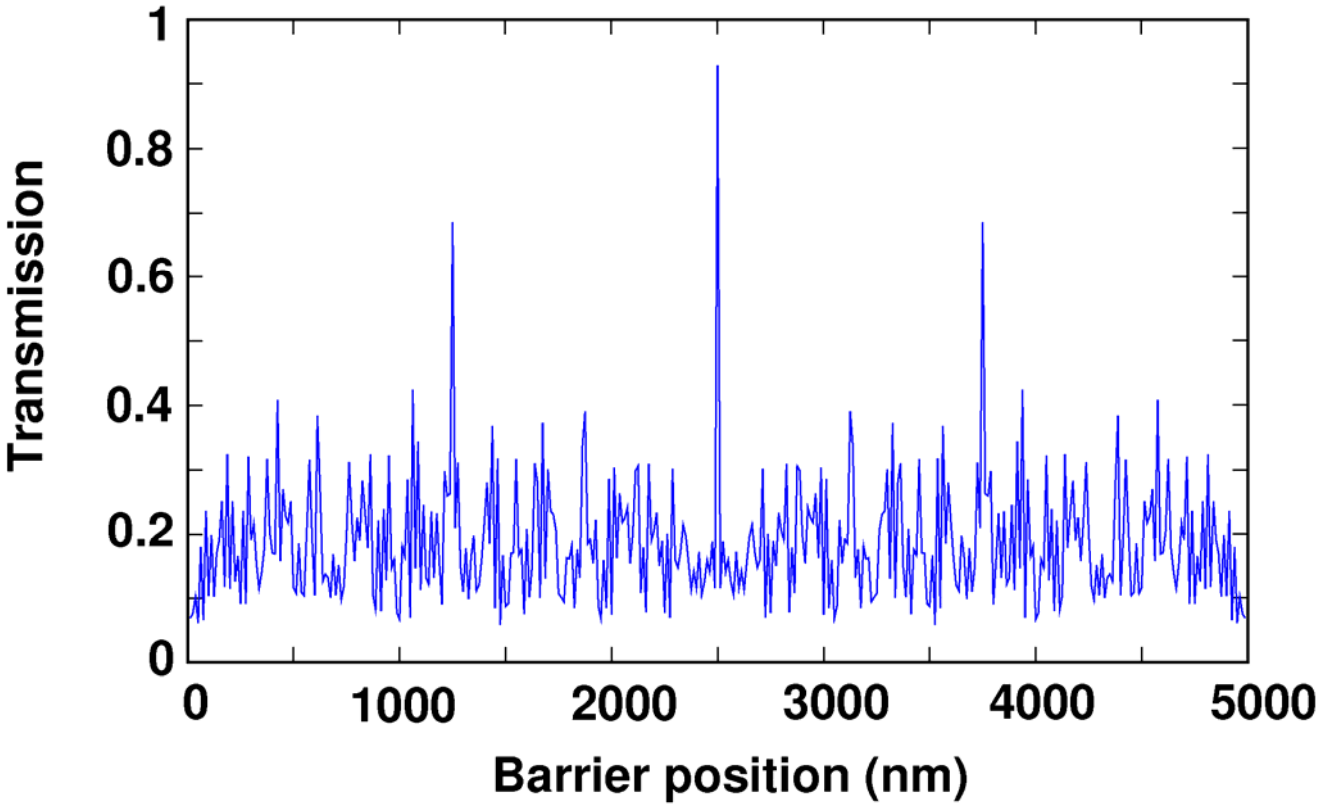


**With a narrower cavity (500 nm) the tunneling enhancement is still observed, with additional features as a function of the barrier position ($T_b$=0.248, $L_b$=10.5 nm)**

# Effect of constriction asymmetry

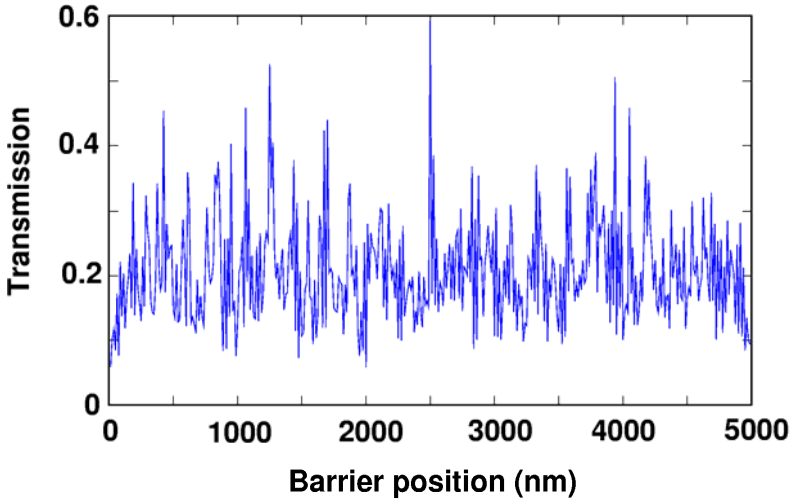


a)

Unequal width

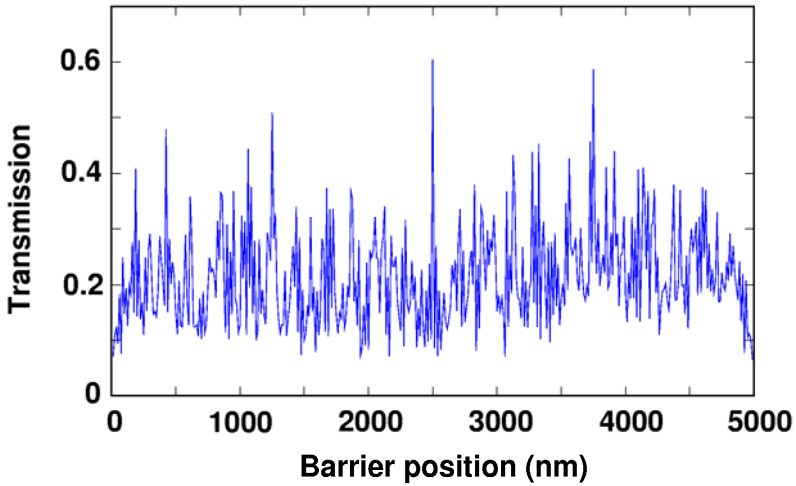


b)

Shifted constrictions

**Also in this case introduction of asymmetries does not destroy the enhancement effect, although some change can be noticed**

# Energy dependence of the tunneling enhancement effect

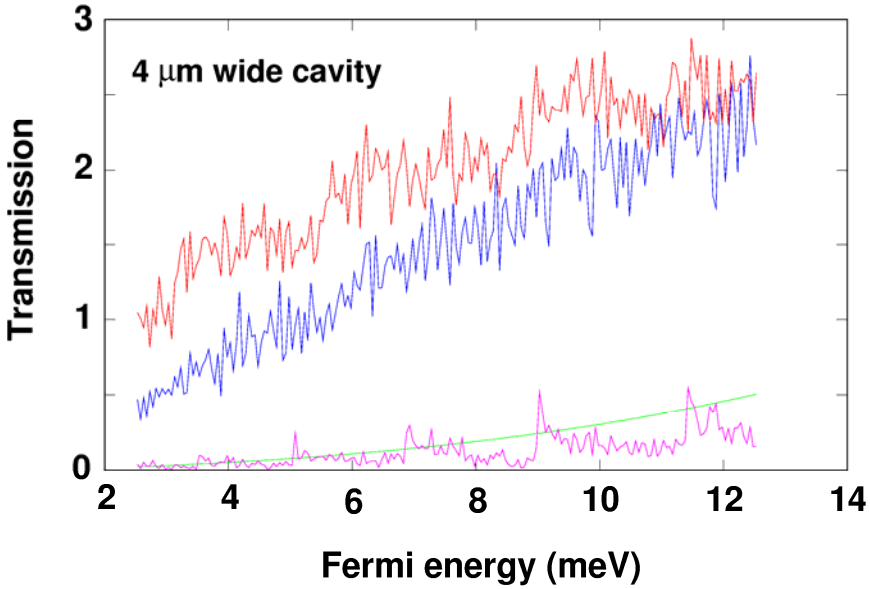


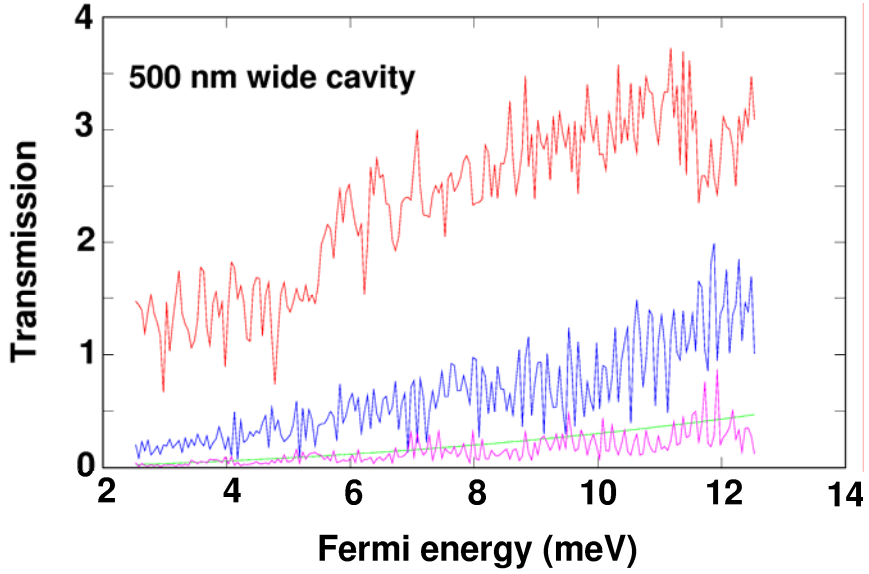


**Further evidence against a resonant origin consists in the energy dependence: the enhancement takes place over a very wide energy range**

# Proposed explanation for the phenomenon

- For narrow enough constrictions the modes inside the cavity are almost identical to those of a closed cavity, therefore all of the even longitudinal modes have a node in the middle
- The enhancement effect gains strength as the width of the constrictions is reduced
- The impinging modes couple with the cavity modes through the constrictions and are transferred into outgoing modes
- A similar argument can be constructed also for the case of a barrier located in other relevant positions, such as 1/4 and 3/4 of the length

# Motivation for noise studies on mesoscopic cavities

- Many results are available in the literature on shot noise suppression in mesoscopic devices: they have been derived with powerful theoretical methods such as random matrix theory and ingenuous semiclassical approaches
- However such methods cannot be straightforwardly applied to generic structures and in some cases their application is so complex that mistakes can occur
- We compare the outcome of our numerical calculations with well established analytical results and with somewhat surprising conclusions in the recent literature
- In particular, we find discrepancies with the findings of S. Oberholzer et al. (Phys. Rev. B, 66, 233304 (2002)) on the shot noise suppression through cascaded cavities
- We instead get good agreement with the experimental data from the measurements by Oberholzer et al. (Nature, 415, 765 (2002)) on shot noise suppression in a cavity threaded by a magnetic field, but we argue for a somewhat different theoretical explanation

# Shot noise in mesoscopic devices

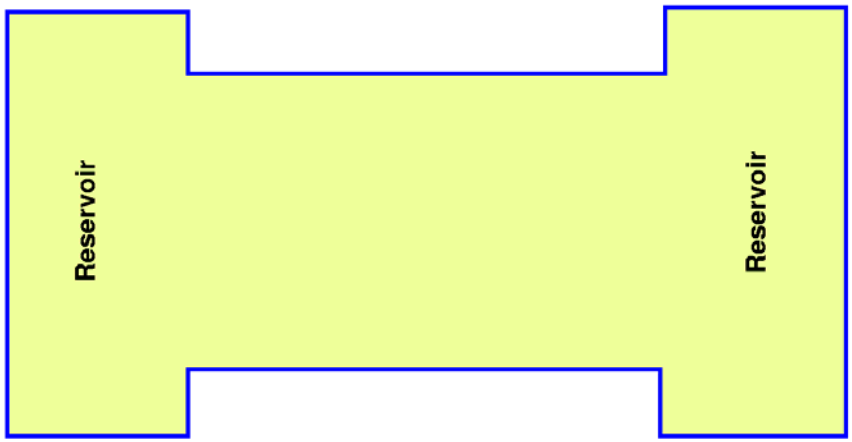


$S_I = 0$

$$S_I = 4\frac{e^2}{h}|eV|\mathrm{Tr}\left[t^\dagger t(I - t^\dagger t)\right]$$

$$S_I = 4\frac{e^2}{h}|eV|\sum_i T_i(1 - T_i)$$

Since, from the Landauer-Büttiker formula,

$$|I| = G|V| = 2\frac{e^2}{h}|V|\sum_i T_i,$$

$$\gamma = \frac{\sum_i T_i(1 - T_i)}{\sum_i T_i}.$$

- Shot noise is the result of the granularity of charge
- In the case of independent electrons, we obtain Schottky's result: ***S***=2***qI***
- In a perfect quantum wire ***S***=0
- In general, shot noise in quantum devices is linked to the transmission eigenvalues (M. Buettiker, Phys. Rev. Lett. 65 (1990))
- The ratio of the actual noise power spectral density to that of full shot noise is defined "Fano factor"

# Averaging techniques

- If many modes are propagating through the device, averaging already takes place over them for each single value of the Fermi energy
- In the case of very few propagating modes and, in particular, of a single propagating mode through part of the structure, the situation is more subtle and averaging over energies must be performed

$$\gamma = \frac{\sum_i T_i(1-T_i)}{\sum_i T_i}$$

$$\gamma = \frac{\langle \sum_i T_i(1-T_i) \rangle}{\langle \sum_i T_i \rangle}$$

# Numerical techniques

- We use different numerical techniques for the evaluation of the transmission matrix, depending on the characteristics of the problem (presence or absence of a magnetic field, size of the device, spatial frequency of the potential fluctuations)
- In the absence of a magnetic field the technique of choice is that of recursive Green's functions
- In the presence of a magnetic field we resort to a recursive scattering matrix technique, with two possible choices of the transverse gauge for the vector potential
- The choice of gauge leads to quite different approaches to the transverse eigenvalue problem

# Recursive Green's functions I

- The simulation domain is filled with a tight-binding square (or cubic) lattice with coupling between nearest neighbors. The domain is then subdivided into sections with constant transverse potential profile and the Green's functions for each of them are computed in the assumption of placing hard walls at both ends.

- Then, coupling between the various sections is treated as a perturbation, via the Dyson equation:

$$\hat{G} = \hat{G}^0 + \hat{G}^0 \hat{V} \hat{G}$$

and a procedure is devised to obtain $G$ for two coupled sections as a function of the $G^0$'s of the uncoupled sections and of the perturbation $\hat{V}$.

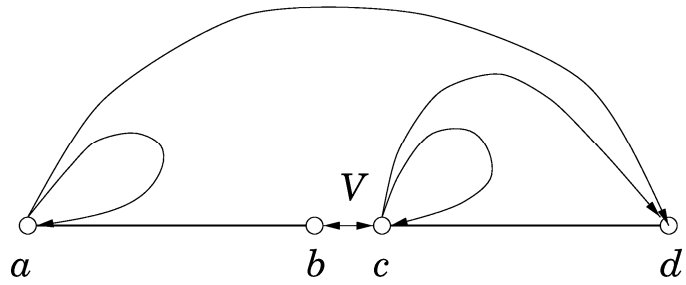

# Recursive Green's functions II

- The procedure is repeated recursively from right to left, until the Green's function from the input to the output of the device is available.

- The elements of $t$, the transmission matrix, are computed from the relationship

$$t_{mn} = -i2V(\sin\theta_n \sin\theta_m)^{1/2} e^{i(\theta_m l - \theta_n j)} \{n|G_{jl}|m\}$$

  and are then used for the calculation of the conductance and of the shot noise power spectral density.

- The Green's function procedure requires as inputs the eigenfunctions and the eigenvalues of each transverse section, that are computed numerically with a finite difference method.

# Computational method I a

One possible choice for the vector potential gauge is the one proposed by Governale and Boese (Appl. Phys. Lett. 77, 3215 (2000)):

$$\overline{A} = \begin{bmatrix} 0 \\ A \\ 0 \end{bmatrix} = \begin{bmatrix} 0 \\ B\,x \\ 0 \end{bmatrix} \quad ,$$

where $x$ is the coordinate along the direction of electron propagation. If the device is subdivided into thin enough slices (each of them should be threaded by a flux less than the flux quantum), the resulting transverse wave functions will be the same as those for the case of $B = 0$, but multiplied by a phase factor:

$$\chi_{n,x_i}(y) = \chi^0_{n,x_i}(y)\, e^{-i\frac{e}{\hbar}A_{x_i} y}.$$

# Computational method I b

- We must consider the propagating modes plus a number of evanescent modes, but device discretization must take into account the requirement over the maximum flux threading each slice:

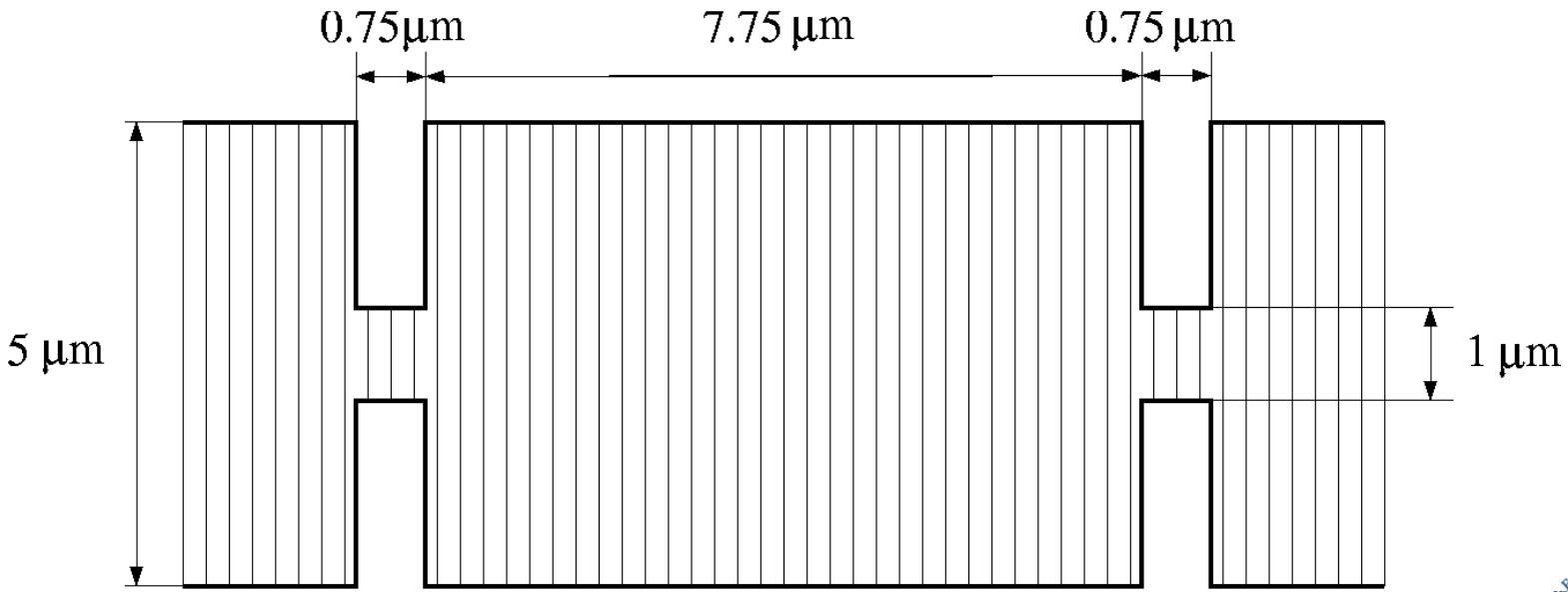

# Computational method II a

Another possible choice for the vector potential gauge is that with a nonzero component along the transverse direction:

$$\overline{A} = \begin{bmatrix} A \\ 0 \\ 0 \end{bmatrix} = \begin{bmatrix} -By \\ 0 \\ 0 \end{bmatrix} \quad ,$$

where $y$ is the transverse coordinate. In this case the Schrödinger equation is not separable and the "transverse wave functions" do depend on the longitudinal wave vector. They can however be expanded in terms of the transverse wave functions for $B = 0$:

$$\Psi(x,y) = \sum_i a_i \exp(ik_{x_i}^+ x) \sum_j c_{ij}^+ \chi_j^0(y) + \sum_i b_i \exp(ik_{x_i}^- x) \sum_j c_{ij}^- \chi_j^0(y) \ ,$$

# Computational method II b

We have computed the expansion coefficients $c_{ij}^{\pm}$ and the longitudinal wave vectors $k_{x_i}^{\pm}$ with the method proposed by Tamura and Ando (Phys. Rev. B **44**, 1792 (1991)). It can be proven that

$$\begin{bmatrix} \mathbf{0} & \mathbf{I} \\ \mathbf{A} & \mathbf{B} \end{bmatrix} \begin{bmatrix} \vec{c}_i^{\,\pm} \\ \vec{d}_i^{\,\pm} \end{bmatrix} = \frac{k_{x_i}^{\pm} W}{\pi} \begin{bmatrix} \vec{c}_i^{\,\pm} \\ \vec{d}_i^{\,\pm} \end{bmatrix} ,$$

where $\vec{c}_i^{\,\pm} = [\, c_{i1}^{\pm}, \ldots, c_{iN}^{\pm} ]^T$ , $\vec{d}_i^{\,\pm} = (k_{x_i}^{\pm} W / \pi)\, \vec{c}_i^{\,\pm}$. The matrices $\mathbf{0}$ , $\mathbf{I}$ , $\mathbf{A}$ and $\mathbf{B}$ have a dimension $N \times N$, with

$$A_{jj'} = \left( \left( \frac{k_F W}{\pi} \right)^2 - \frac{E_j}{E_1^*} \right) \delta_{jj'} - \left( \frac{\hbar \omega_c}{2 E_1^*} \right)^2 \langle\, \chi_j^0 \mid \left( \frac{\pi y}{W} \right)^2 \mid \chi_{j'}^0 \,\rangle ,$$

while

$$B_{jj'} = \frac{\hbar \omega_c}{E_1^*} \langle\, \chi_j^0 \mid \left( \frac{\pi y}{W} \right) \mid \chi_{j'}^0 \,\rangle .$$

# Computational method II c

- In this case slice length is limited only by the extension of sections with constant transverse potential, but a very large basis may be needed for the expansion of the transverse wave functions

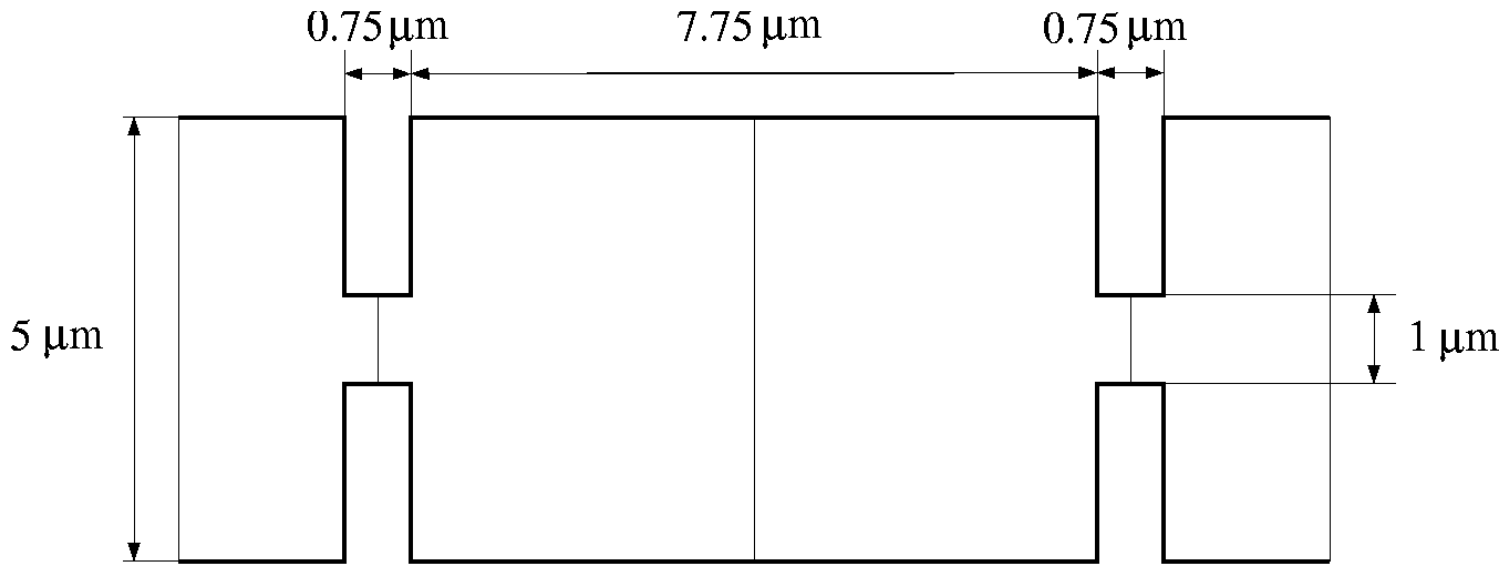

# Noise for *B*=0

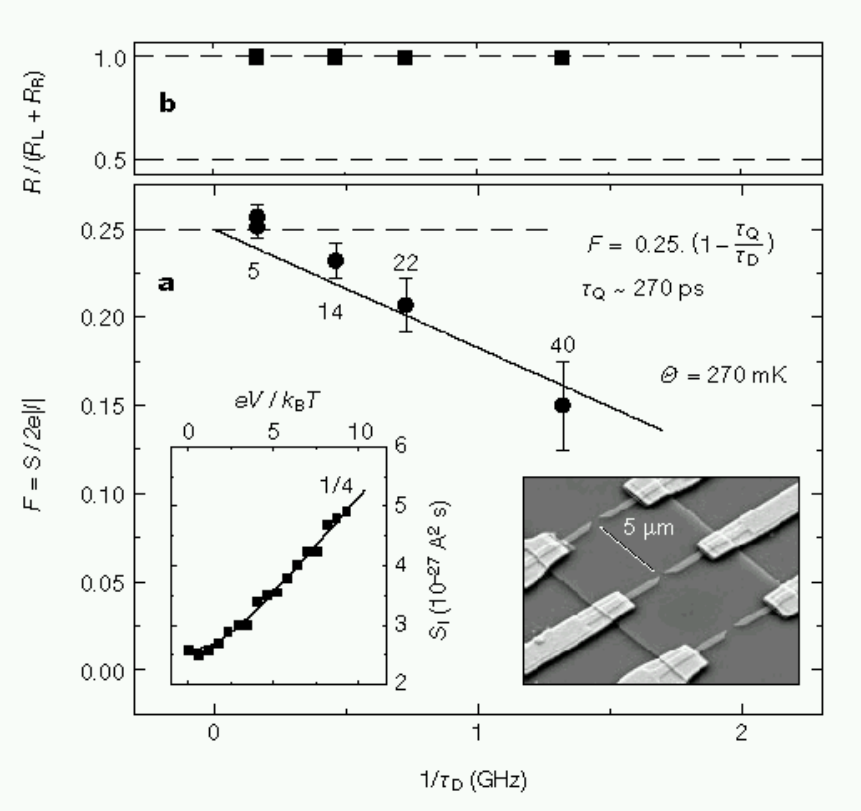


S. Oberholzer, E. V. Sukhorukov, C. Schönenberger, Nature 415, 765 (2002)

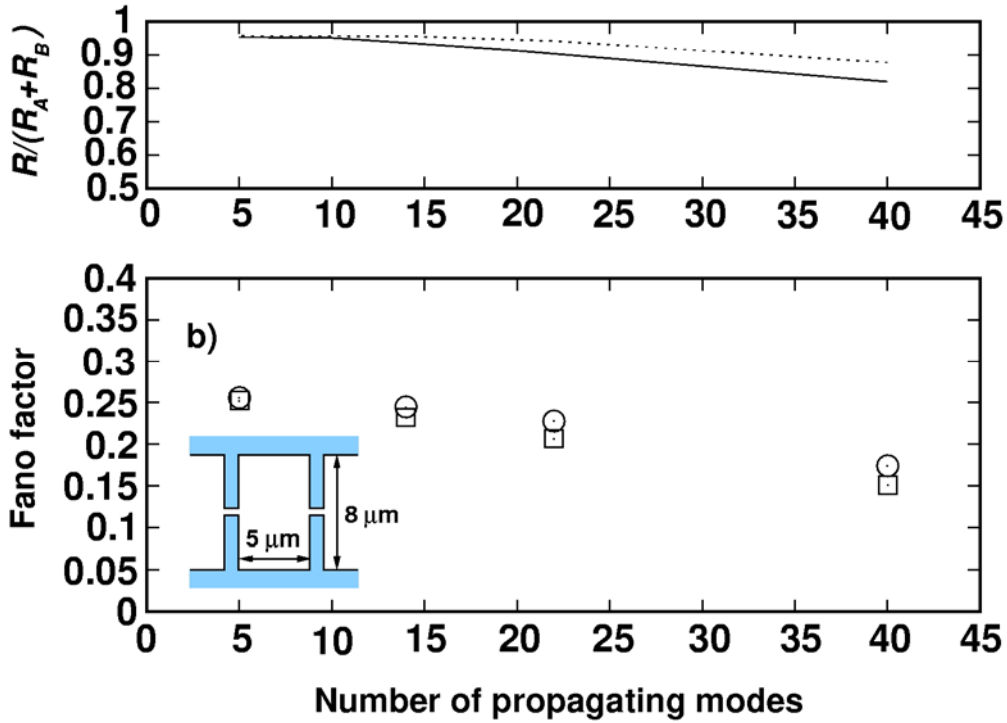


P. Marconcini, M. Macucci, G. Iannaccone, B. Pellegrini, G. Marola, Europhys. Lett. 73, 574 (2006)

# Cavity conductance

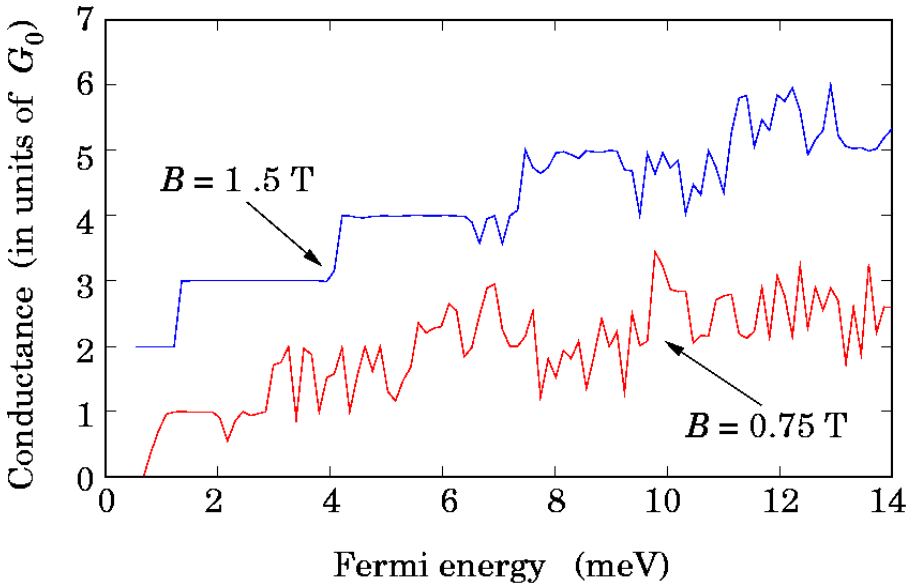


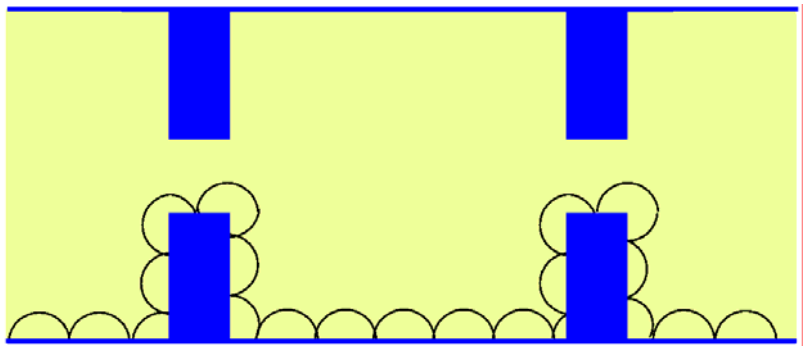

$W$=100 nm

- For B=0, the resistances of each constriction add up, and conductance quantization is washed out
- As B is increased, conductance quantization is recovered and the resistance of the cavity equals that of a single constriction
- This can be easily understood if we consider that, as the cyclotron radius becomes smaller than the aperture widht, edge states may flow freely through the cavity
- This calculation has been performed with the gauge with a nonzero longitudinal component

# Noise as a function of magnetic field

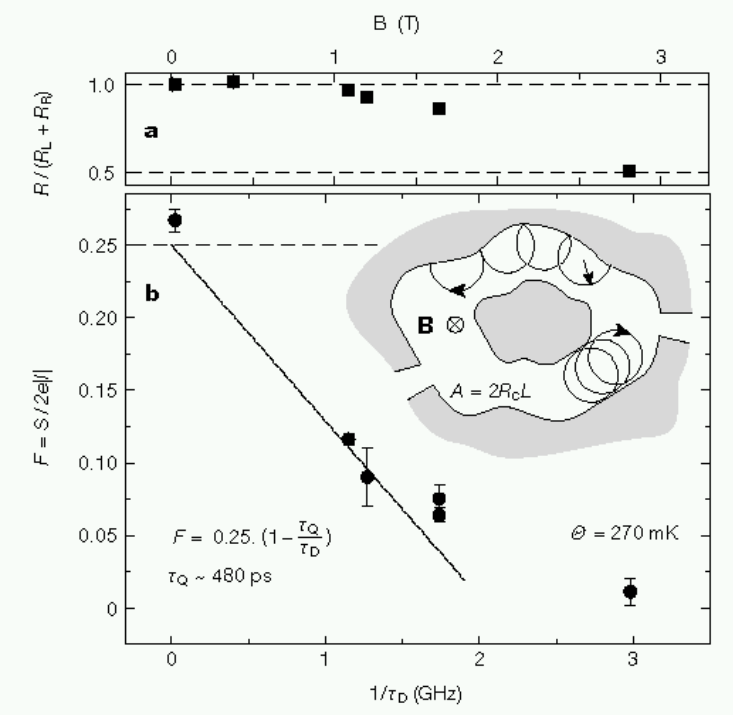


S. Oberholzer, E. V. Sukhorukov, C. Schönenberger, Nature 415, 765 (2002)

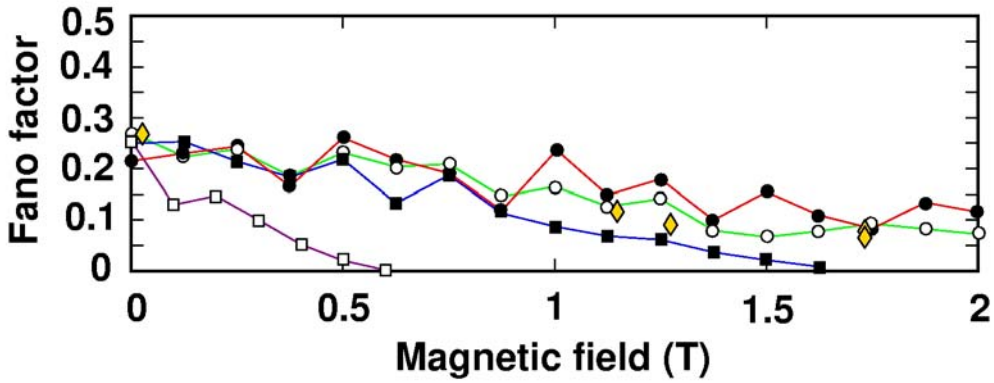


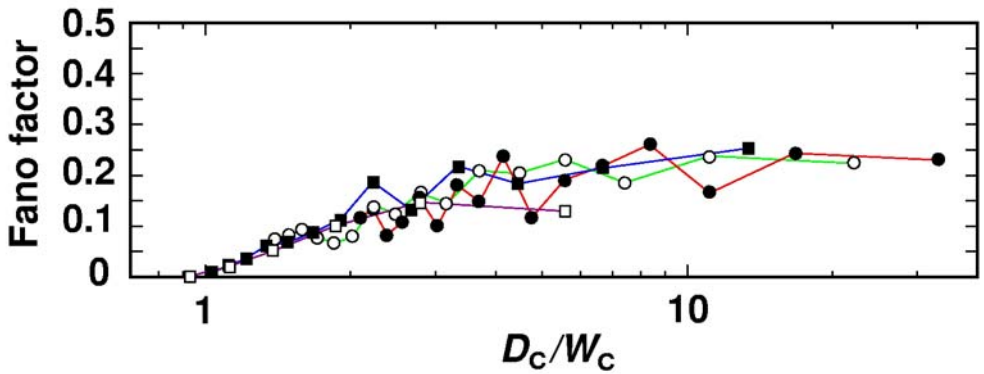


P. Marconcini, M. Macucci, G. Iannaccone, B. Pellegrini, G. Marola, Europhys. Lett. 73, 574 (2006)

# Evaluation of the cyclotron radius

- The Fermi energy in the device is, according to Oberholzer et al. (PRL 86, 2114 (2001)), 9.14 meV. From this we get a cyclotron radius at 1 T of

$$R_c = \frac{\sqrt{2mE_f}}{eB} = 83.4\,\mathrm{nm}$$

- Therefore we expect significant noise suppression to be observable at 1 T for constriction widths of the order of about 85 nm
- This approach does not require any fitting parameter

# $B$=0

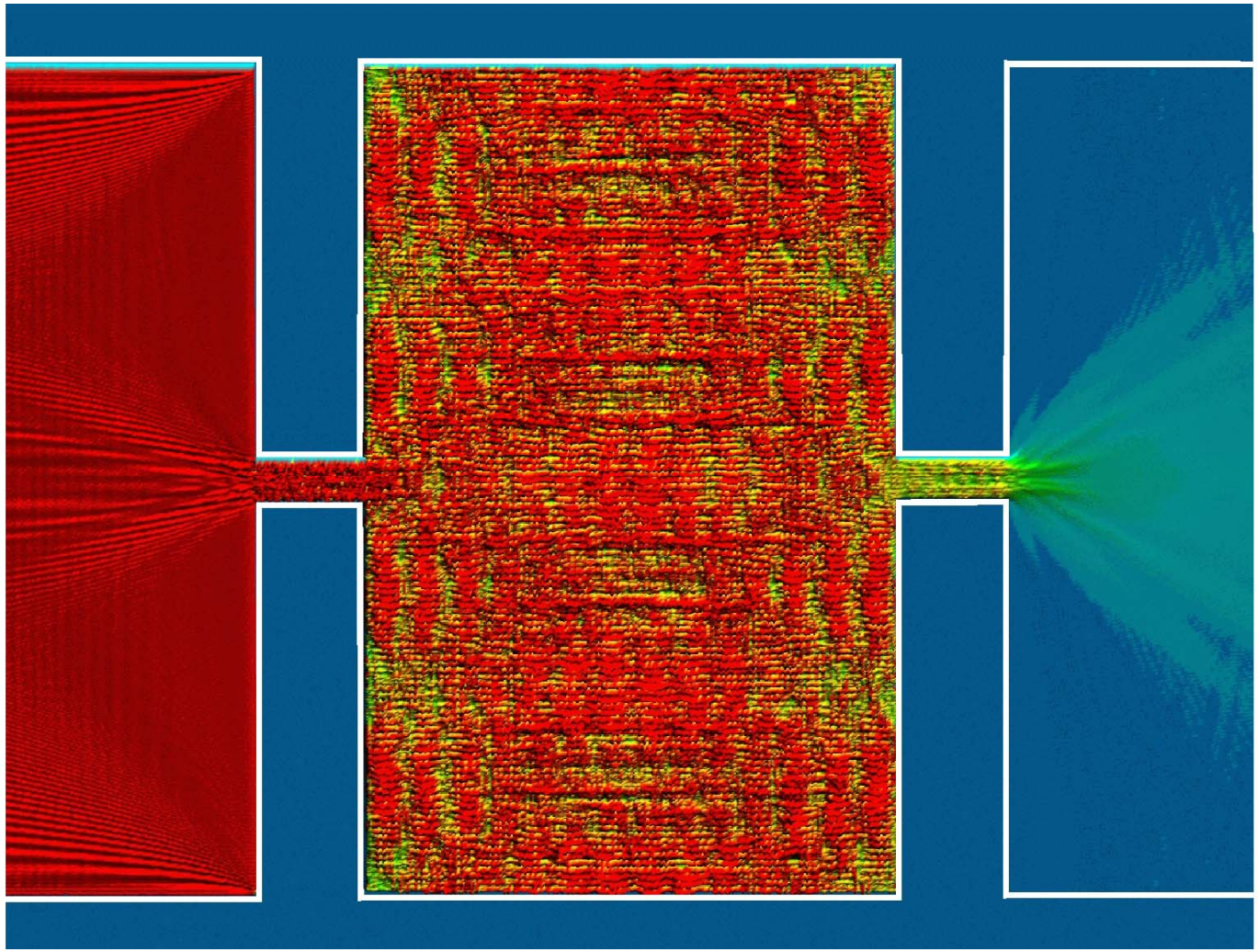

# Intermediate *B*

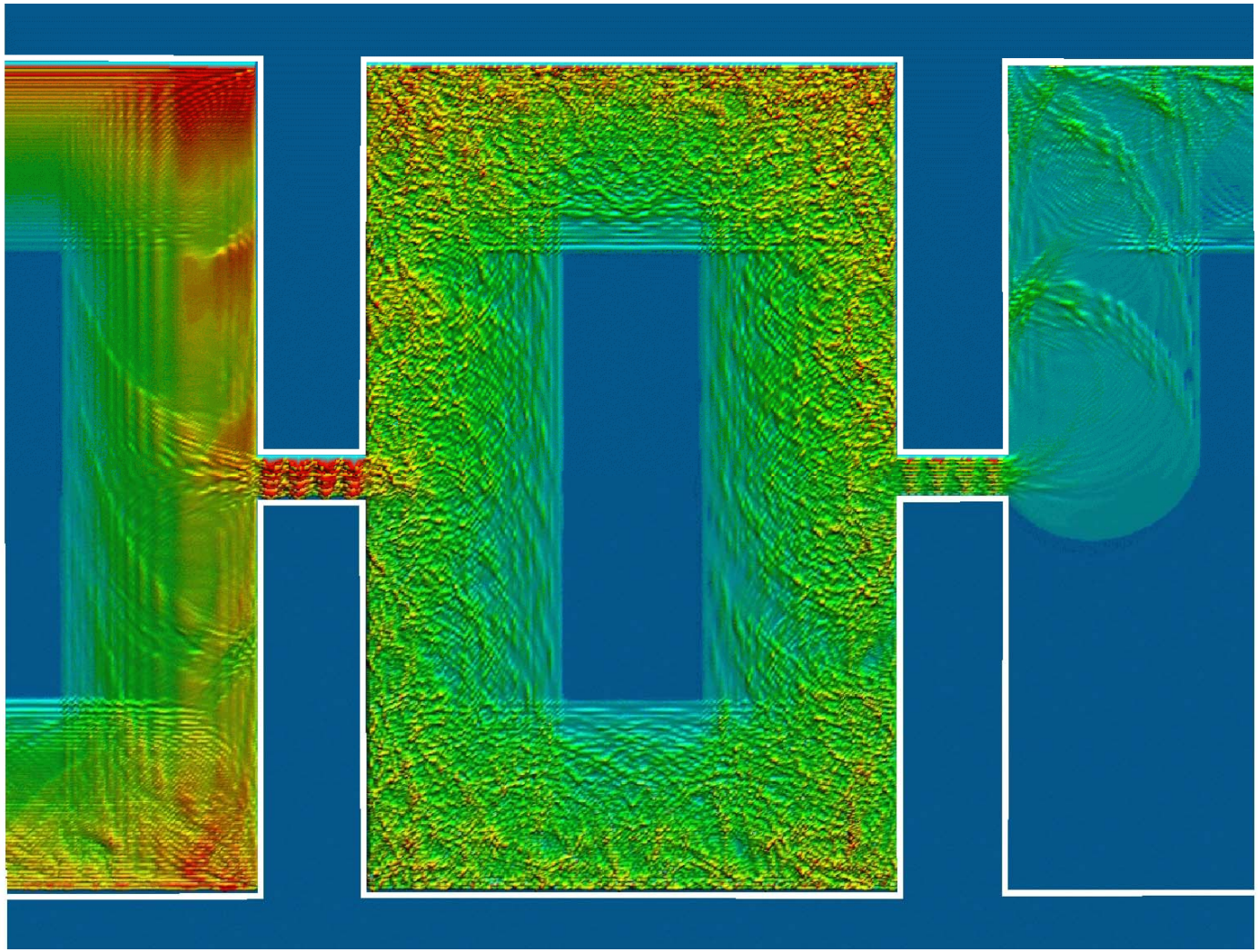

# Large *B*

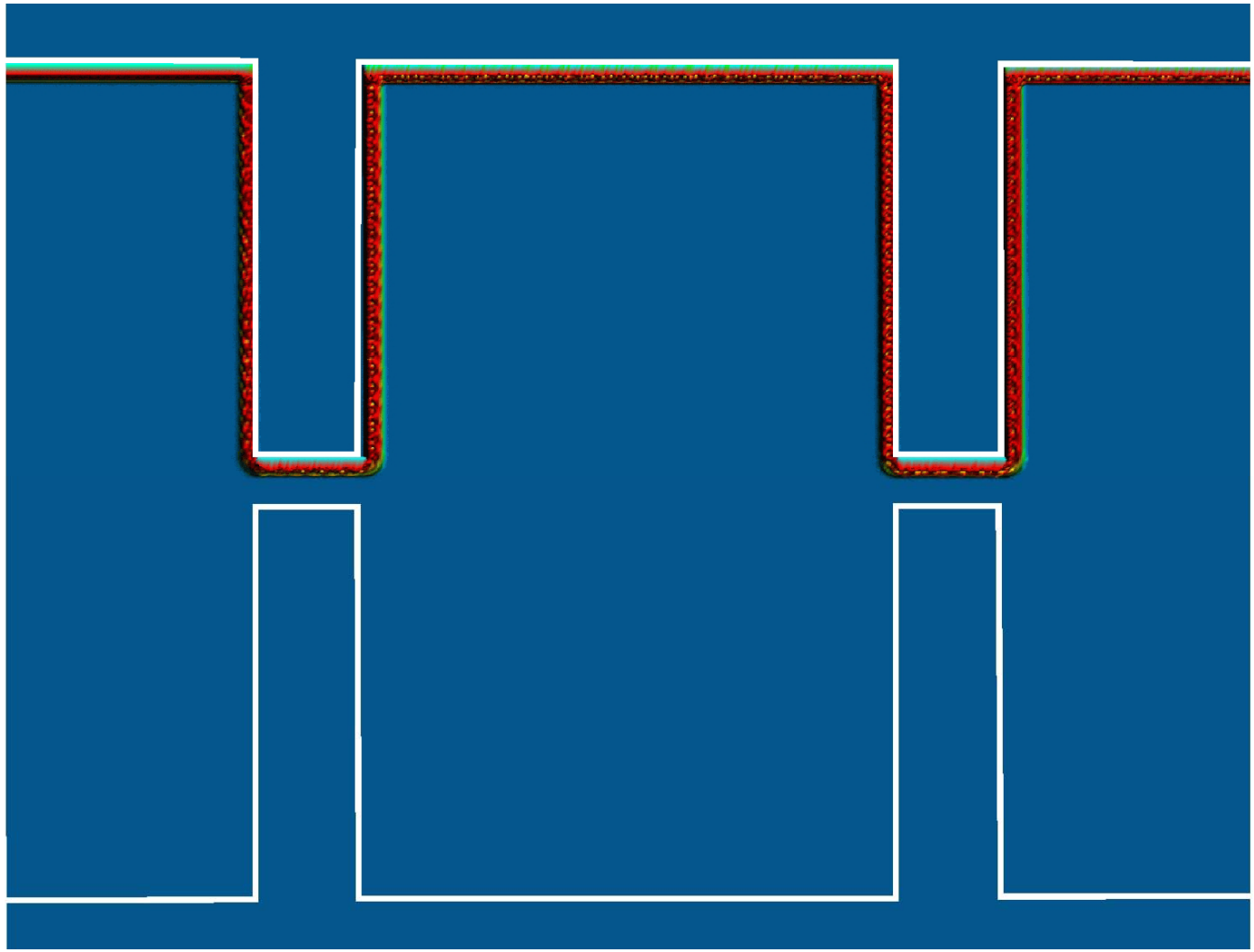

# Cavity with a barrier I

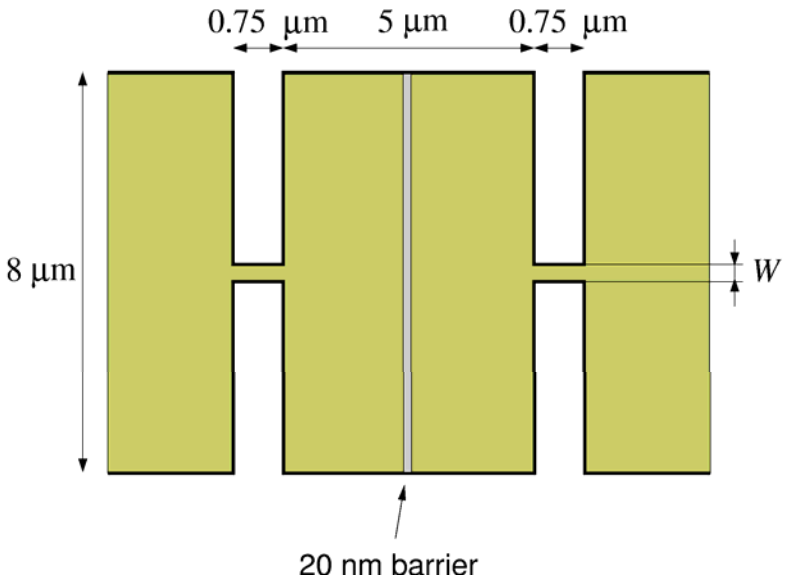


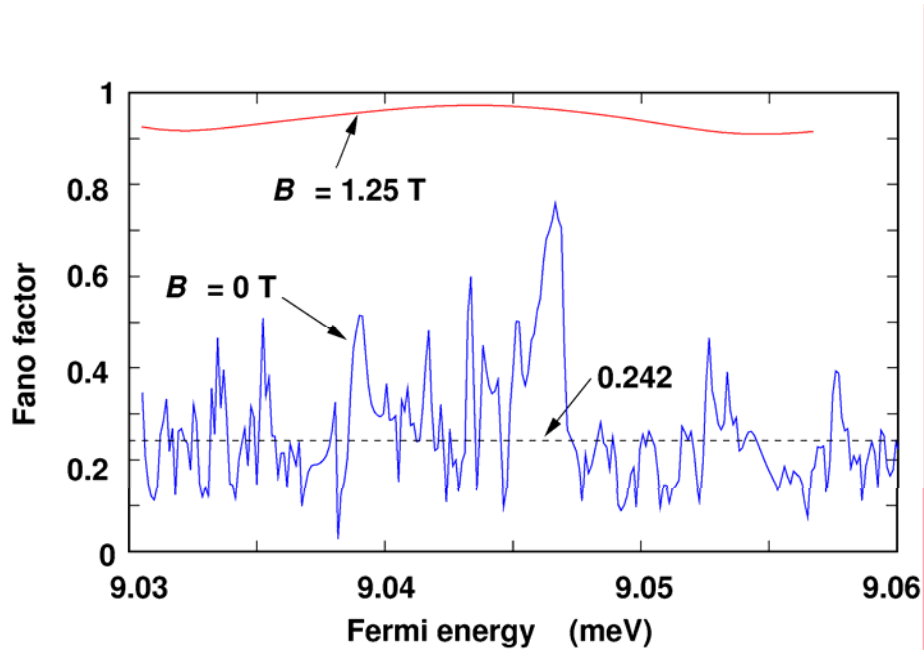


- If a potential barrier with low transmission is included in the cavity, the Fano factor for *B*=0 is unaffected, while for *B* large enough that the cyclotron radius is smaller than the apertures, the Fano factor approaches unity

# Cavity with a barrier II

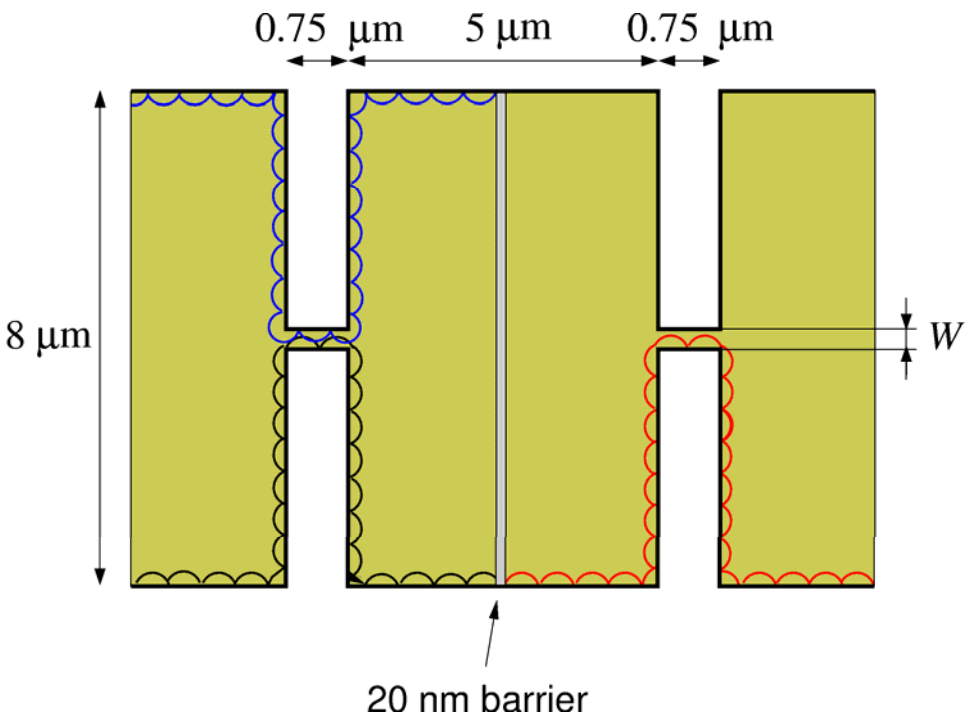


- For a value of B such that the cyclotron radius is smaller than the apertures, edge states flow unimpeded at the entrance of the cavity and scatter against the potential barrier
- Reflected electrons exit the cavity through the entrance while transmitted electrons reach the exit without further scattering
- The overall structure thus behaves, from the noise point of view, as if there were no cavity

# Cavities with different shapes

Rectangular cavity with adiabatic constrictions

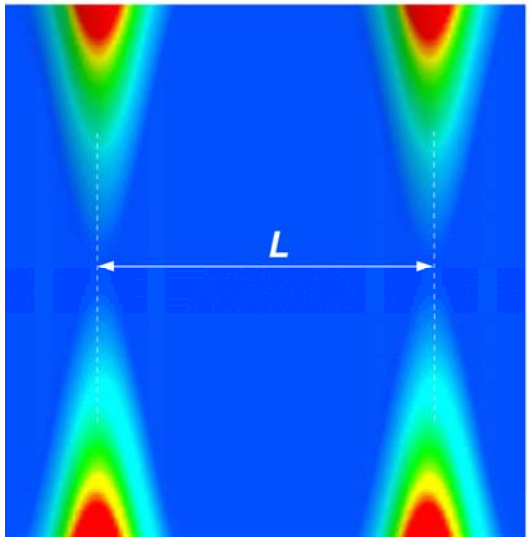


Stadium shaped cavity

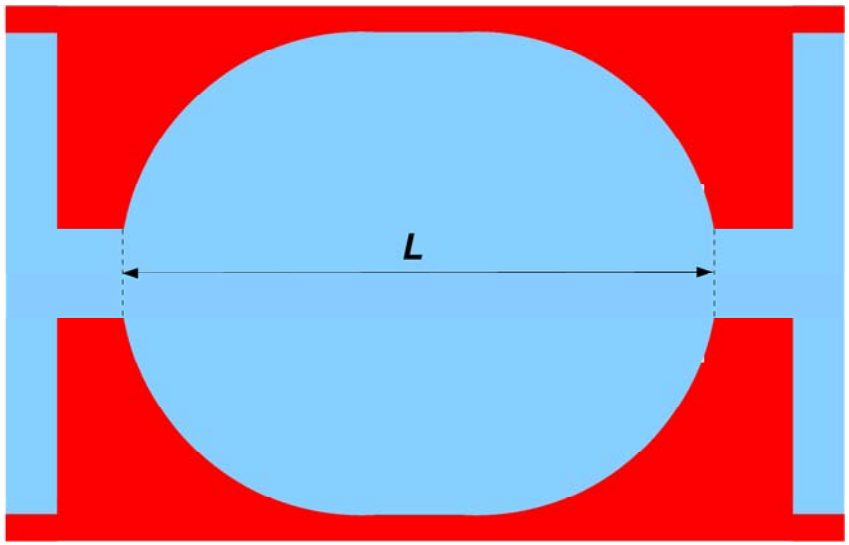


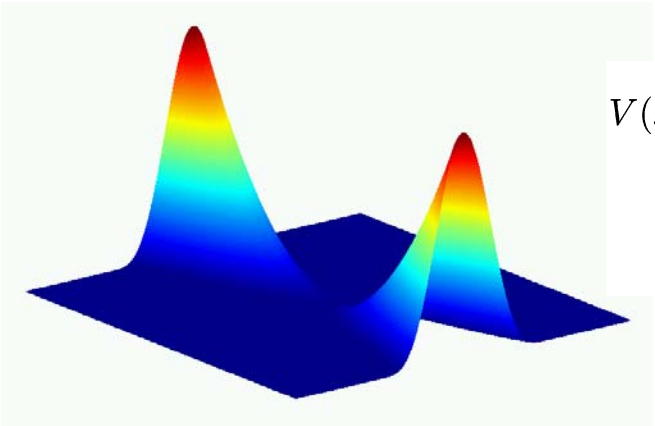

$$V(x,y) = \frac{E_1}{2}\left[1+\cos\left(\frac{2\pi x}{L_x}\right)\right] + E_2 \sum_{\pm}\left(\frac{y-y_{\pm}(x)}{\Delta}\right)^2 \theta[\pm(y-y_{\pm}(x))]$$

$$y_{\pm}(x) = \pm\frac{L_y}{4}\left[1-\cos\left(\frac{2\pi x}{L_x}\right)\right]$$

# Cavities with narrow constrictions

- We have found that, in the case of constrictions that are narrow with respect to the width of the cavity, its length does not affect the Fano factor.
- This is true both in the absence of a magnetic field (with a Fano factor of 1/4) and in the presence of a magnetic field (with a Fano factor below 1/4).

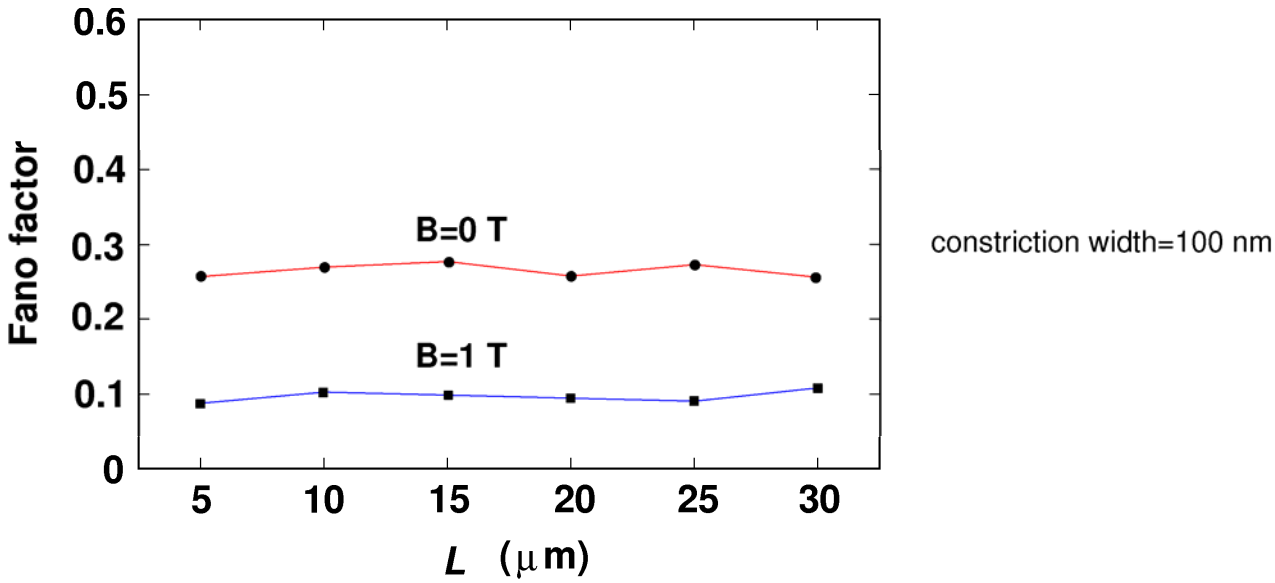

# Cavities with wide constrictions and B=0

- If the width of the constrictions is not small in comparison with the cavity width, in the absence of magnetic field the Fano factor, starting from a value below 1/4, increases as the length of the cavity is increased, apparently up to an asymptotic value.
- There is little difference between the results obtained for cavities with different shapes.

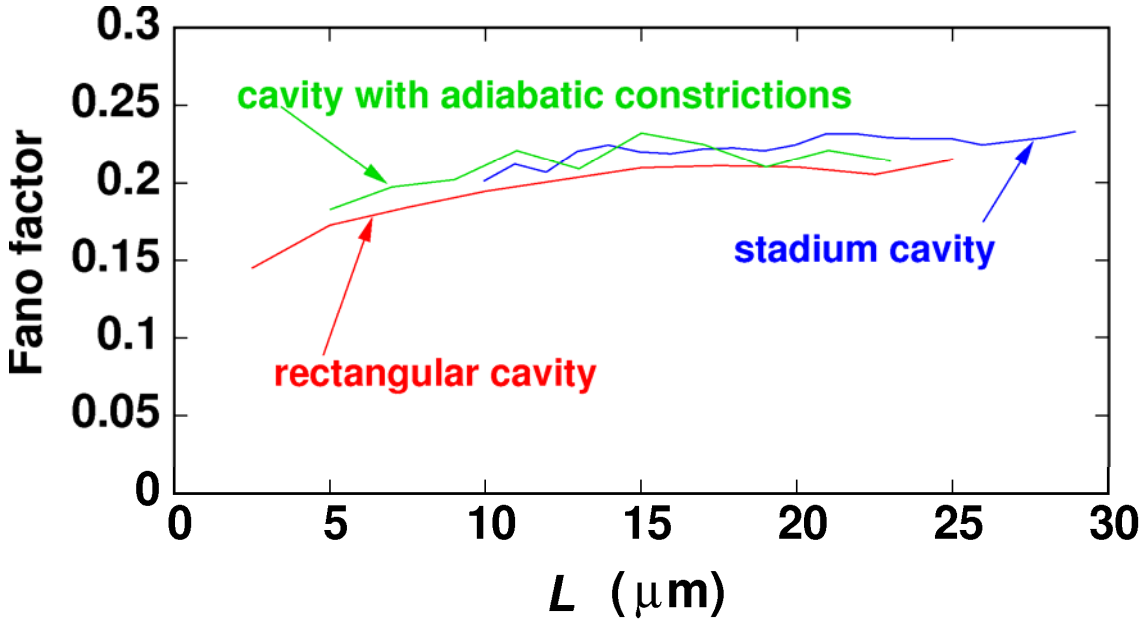


number of modes propagating in each constriction: 40

# Cavities with wide constrictions and B≠0

- In the presence of a sufficiently high magnetic field, we find that also if the constrictions are wide the Fano factor is independent of the cavity length.

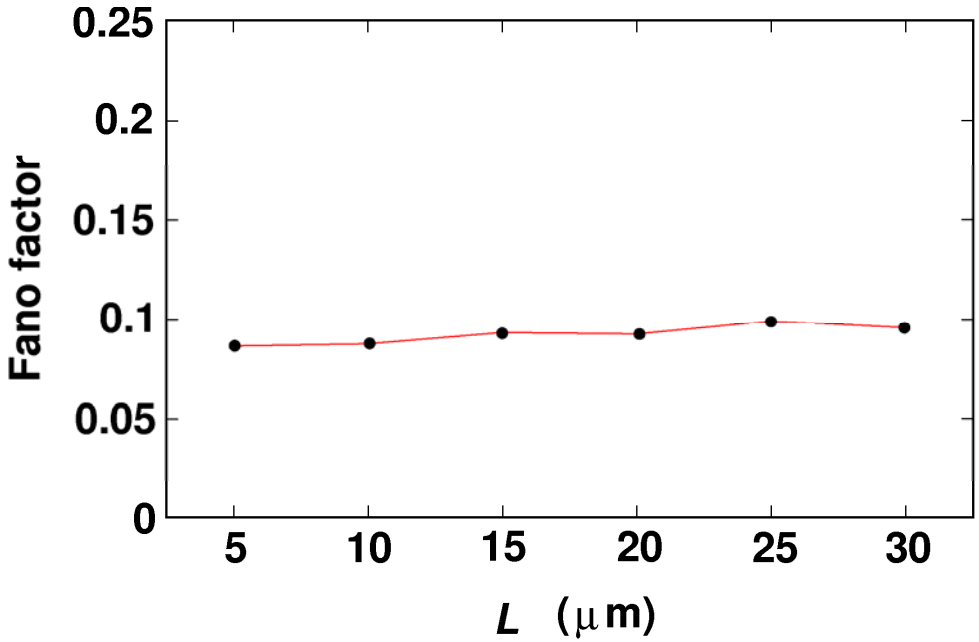


constriction width=500 nm

B=0.15 T

# Cavities with wide constrictions

- In particular, starting from the behaviour observed in the absence of magnetic field, as $B$ is increased the Fano factor dependence on the cavity length appears to decrease (although some fluctuations are observed for intermediate values of $B$), until, above a threshold value, it vanishes.

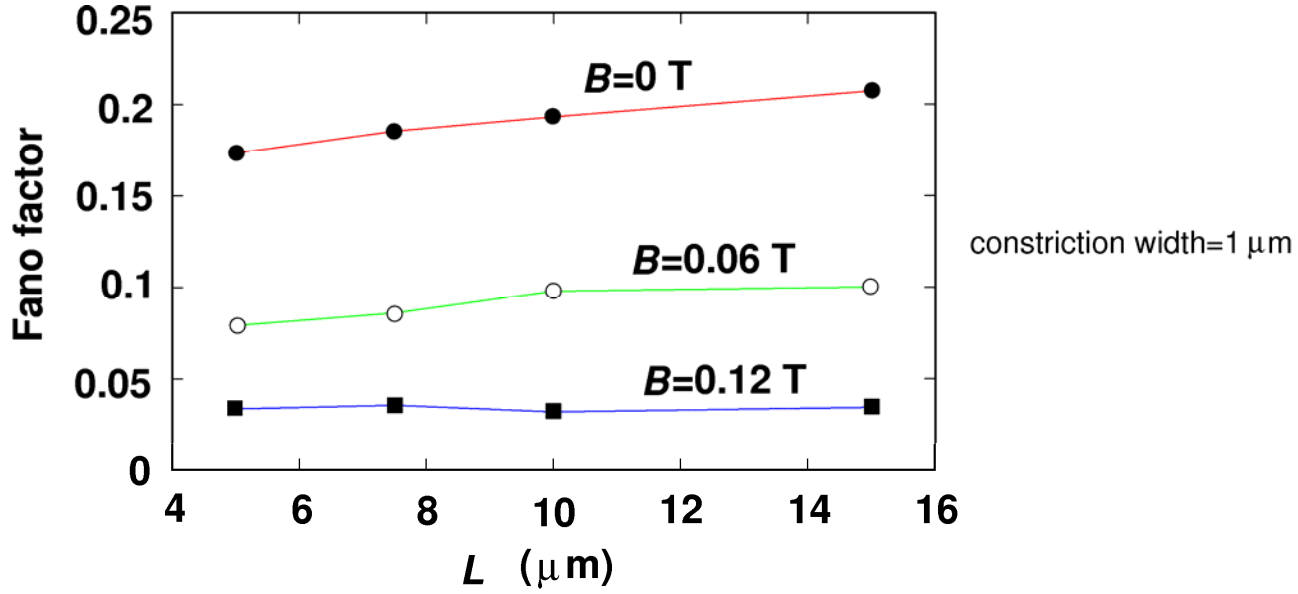

# Noise dependence on cavity area

- No significant dependence of the Fano factor on cavity area is observed

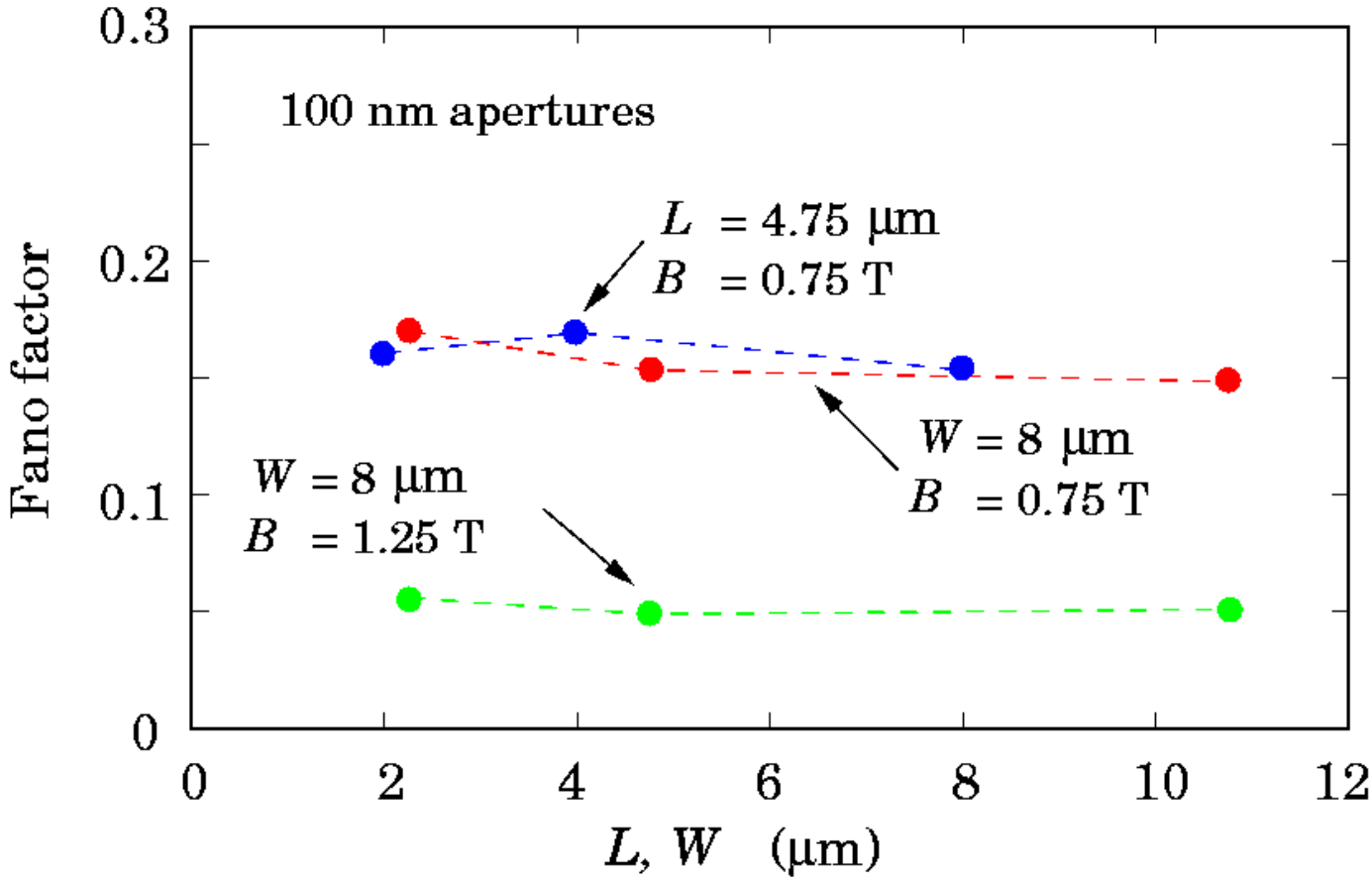

# Electron density in identical cascaded cavities

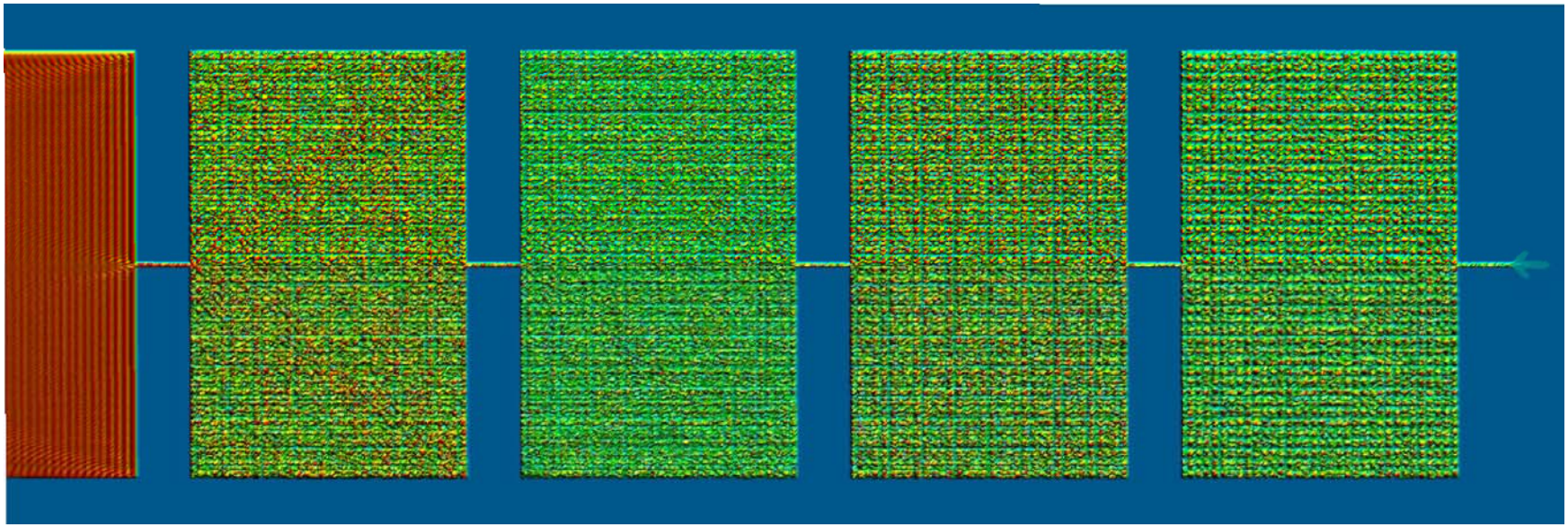

**There is no apparent "beaming" effect: a uniform texture is visible, with features on the scale of the Fermi wavelength**

# Identical cascaded cavities

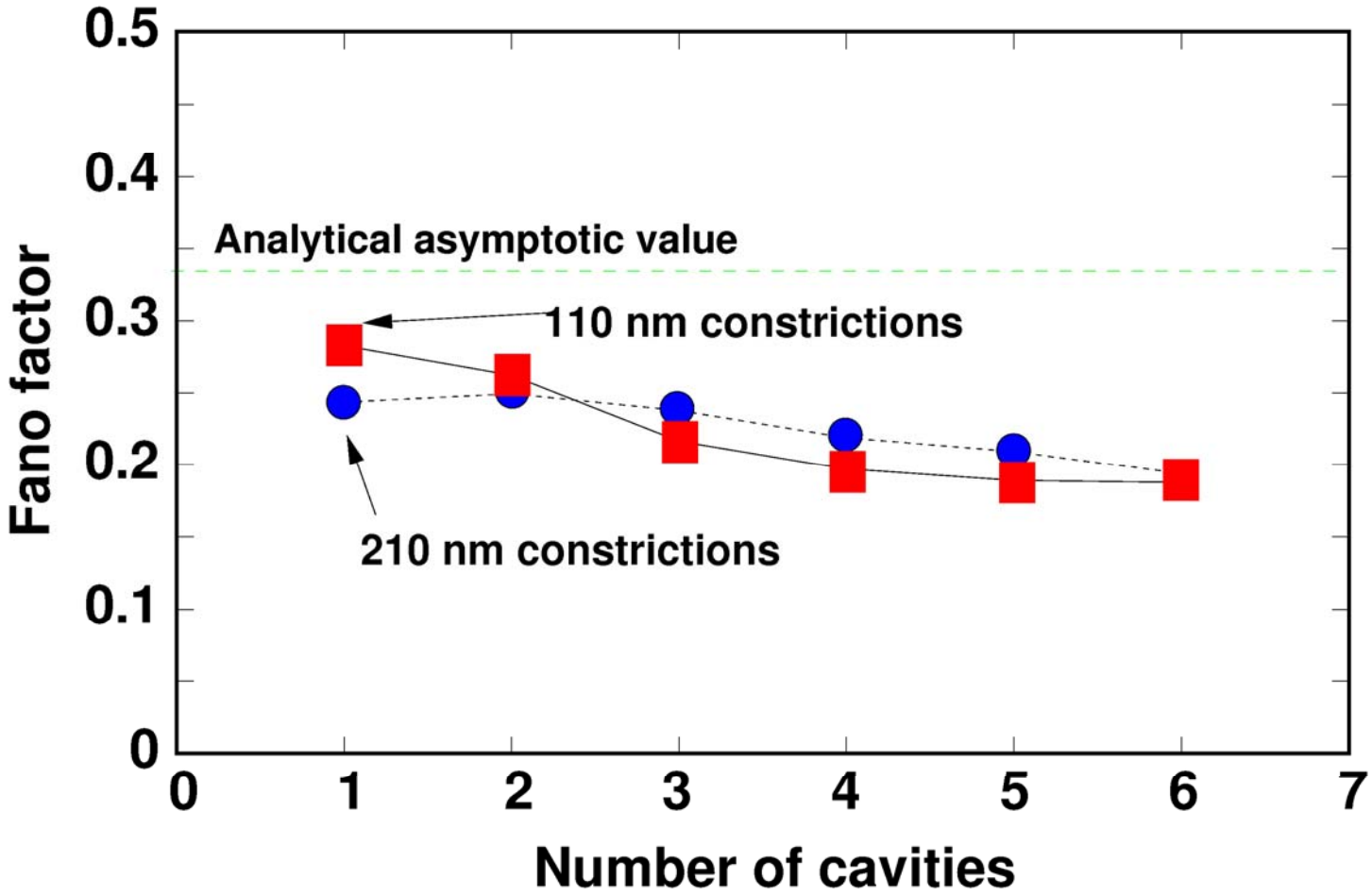

# Cascaded unequal cavities

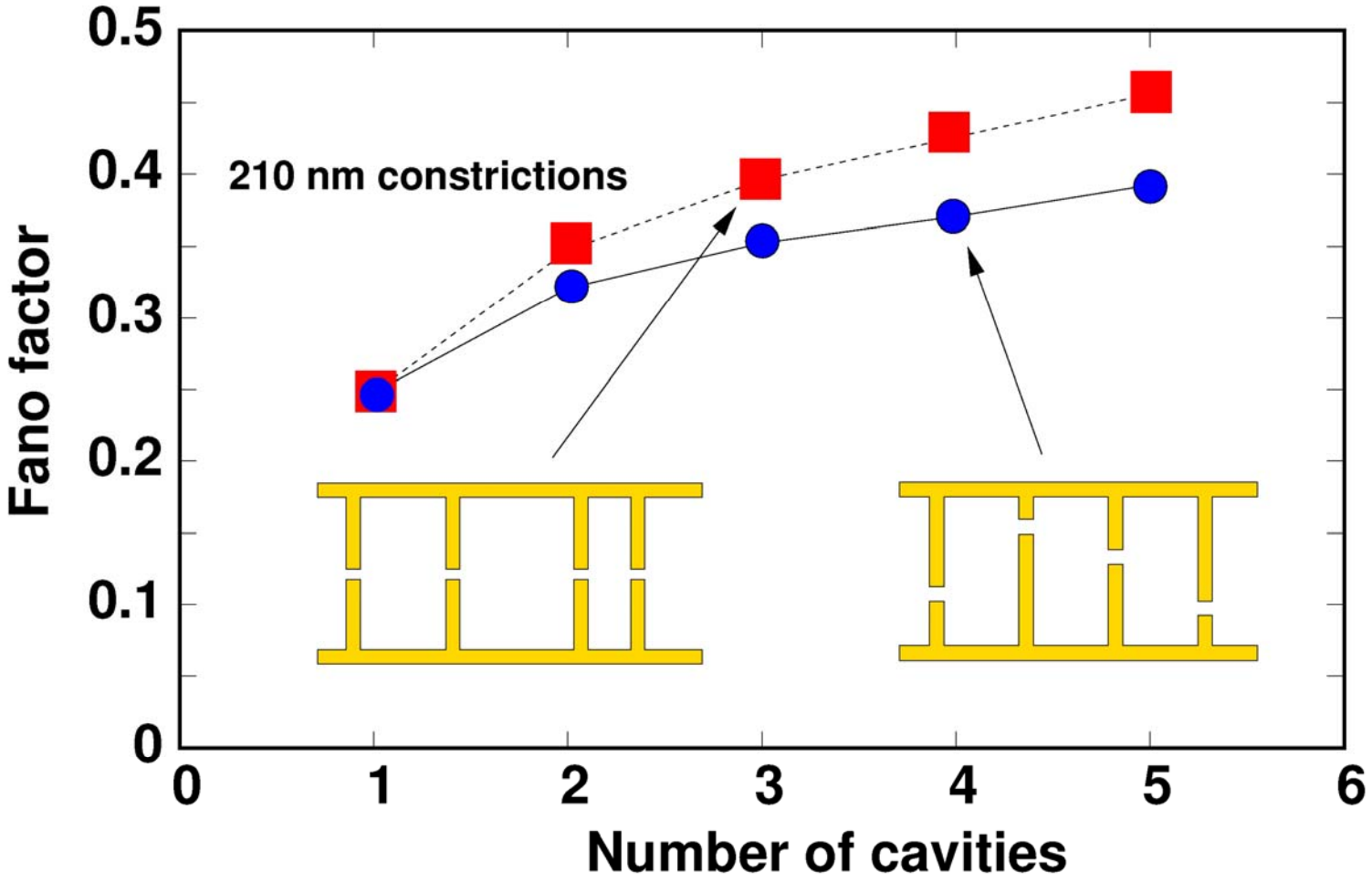

# Resistance of cascaded cavities

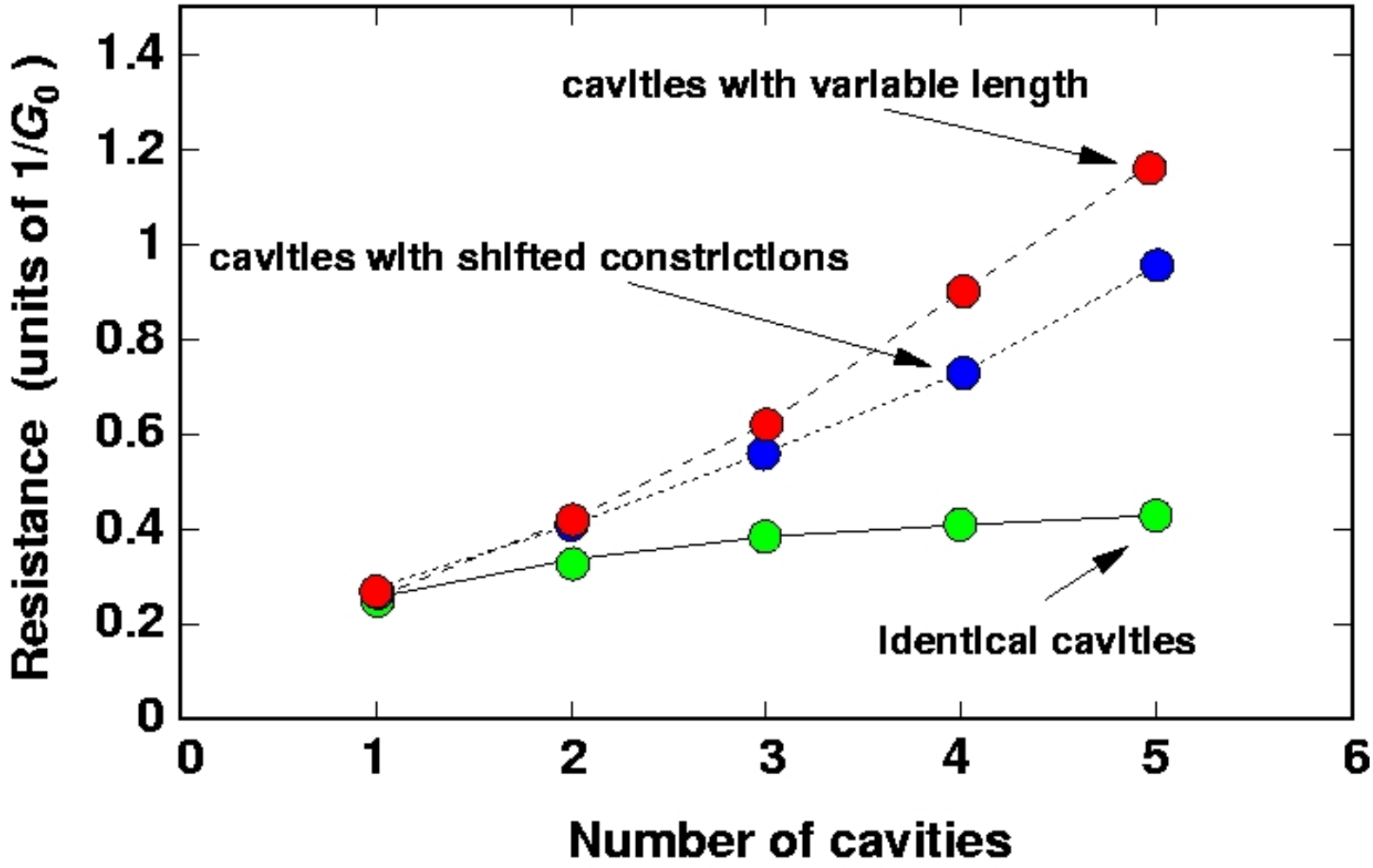

# Conclusions

- A non-resonant tunneling enhancement due to a mesoscopic cavity appears if a barrier is placed in specific positions and can be explained with a simple approximate argument
- Numerical modeling tools are instrumental in the interpretation of experimental data
- Good agreement has been obtained with available experimental results on the Fano factor in a cavity threaded by a perpendicular magnetic field
- The Fano factor for a cavity containing a potential barrier has been investigated, and the results have been explained on the basis of an intuitive model
- Shot noise suppression in cascaded cavities is found to vary little with respect to the case of  a single cavity if they are identical
- If cascaded cavities are not identical, some of the results from existing semiclassical models are recovered, but further work is needed to understand the origin of the difference with respect to the case of identical cavities